We are IntechOpen,
the world's leading publisher of
Open Access books
Built by scientists, for scientists

4,800
Open access books available

122,000
International authors and editors

135M
Downloads

Our authors are among the

154
Countries delivered to

TOP 1%
most cited scientists

12.2%
Contributors from top 500 universities

CLARIVATE ANALYTICS
BOOK
CITATION
INDEX
INDEXED

WEB OF SCIENCE™

Selection of our books indexed in the Book Citation Index
in Web of Science™ Core Collection (BKCI)

Interested in publishing with us?
Contact book.department@intechopen.com

Numbers displayed above are based on latest data collected.
For more information visit www.intechopen.com

Finite Element Modeling and Simulation of Healthy and Degenerated Human Lumbar Spine

Márta Kurutz[1] and László Oroszváry[2]
[1]Budapest University of Technology and Economics,
[2]Knorr-Bremse Hungaria Ltd, Budapest,
Hungary

1. Introduction

Numerical analyses are able to simulate processes in their progress that are impossible to measure experimentally, like aging and spinal degeneration processes. 3D finite element (FE) simulations of age-related and sudden degeneration processes of compression-loaded human lumbar spinal segments and their weightbath hydrotraction treatment are presented here. The goal is to determine the effect of the main mechanical degeneration parameters on the deformation and stress state of the lumbar functional spinal units (FSU) during long- and short-term degeneration processes. Moreover, numerical analysis of the effect of the special underwater traction method, the so-called weightbath hydrotraction therapy (WHT) for treating degenerated lumbar segments is also presented in this chapter.

About 60-85 % of the human population is afflicted by lumbar disc diseases, by low back pain (LBP) problems, most of them the young adults of 40-45 years, due to the degeneration of the lumbar segments. Degeneration means an injurious change in the structure and function of FSU, caused by normal aging or by sudden accidental, often unexpected effects yielding mechanical overloading. Degeneration starts generally in the intervertebral discs: in the central kernel of it, in the nucleus pulposus. Aging degeneration of the disc is manifested in loss of hydration, a drying and stiffening procedure in the texture of nucleus, and a hardening of annulus as well, accompanied by the appearance of buckling, lesions, tears, fiber break in the annulus or disruption in the endplates, collapse of osteoporotic vertebral cancellous bone (Adams et al., 2002). Sudden accidental degeneration of overload yields the instant loss of hydrostatic compression in nucleus, accompanied or due to some other failures mentioned above. Several recent studies concluded that light degeneration of young discs leaded to instability of lumbar spine and the stability restored with further aging (Adams et al., 2002; Rohlmann et al., 2006), however, sudden accidental degeneration may be also dangerous in young age, thus, the present study aims to understand the biomechanical function of these degeneration processes.

The first goal of this study was to obtain numerical conclusions for the mechanical effects of age-related and sudden degeneration processes of the lumbar spine under compression. The

question is answered also why the young adults of 40-45 years have the most vulnerable lumbar discs, and why increases the stability of lumbar segments with further aging.

On the other hand, for the degenerated lumbar spine, for the LBP problems, traction might be an effective treatment. Traction treatments have been well-known for a long time, however, as often happens, instead of stress relaxation, the compression increases in the discs due to the muscle activity (Andersson et al., 1983; White and Panjabi, 1990; Ramos and Martin, 1994). These observations verify the importance of the special Hungarian traction method, the so-called weightbath hydrotraction therapy (WHT), introduced by Moll (1956, 1963), indications and contraindications described by Bene (1988). In WHT patients are suspended in water on a cervical collar for a period of 20 minutes, loaded by extra lead weights on ankles, when the patients are practically in sleeping position in the lukewarm water with completely relaxed muscles. WHT consists of instant elastic and viscous creeping phases. In this study the elastic phase will be analyzed. As far as the authors know, finite element analyses of lumbar FSUs in pure axial tension without the effect of muscles cannot be found in the literature. As White and Panjabi (1990) and Bader and Bouten (2000) established, tensile stresses and deformations are analyzed associated with flexion and extension only, without mentioning axial tension as a dominating loading effect.

Thus, in this study, the latter case will be analyzed. By means of this study of WHT, the beneficial clinical impacts of the treatment are supported by numerical mechanical evidences.

2. Short structural anatomy of the lumbar spine and spine segments

The lumbar spine is the section of spinal column between the thorax and the sacrum. It consists of five *vertebrae* named L1 to L5 with their *posterior elements* and *articular facet joints*, of *intervertebral discs*, *ligaments* and the surrounding *muscles*. The clinical anatomy of the lumbar spine can be studied in the books of Bogduk and Twomey (1987), White and Panjabi (1990), Dvir (2000), Benzel (2001) and Adams et al. (2002).

The lumbar *vertebrae* are quasi cylindrical with a lateral width of 40-50 mm and sagittal depth of 30-35 mm. The height of a lumbar vertebra is about 25-30 mm. The lumbar vertebrae are thicker anteriorly than posteriorly resulting in anteriorly convex curvature of the spine known as the lumbar lordosis. The *vertebral body* consists of an outer shell of high strength *cortical bone* and of the internal *cancellous bone* as a network of vertical and horizontal bone struts called trabeculae. The superior and inferior surface of the vertebral body is covered by the *bony endplates* of thin cortical bone perforated by many small holes as the passage of metabolites from bone to the discs. Towards the upper end of the posterior surface of the vertebral body the pedicles support the posterior elements, the lamina the neural arch, the vertebral foramen, the spinous process, the transverse processes, the superior and inferior articular processes, the synovial joints called articular facet joints.

The *intervertebral discs* separate the adjacent vertebrae. They are quasi cylindrical with a lateral width of 40-45 mm and sagittal depth of 35-40 mm. The height of the lumbar disc is about 10 mm. The disc consists of three components: the nucleus pulposus, the annulus fibrosus and the superior and inferior endplates. The *nucleus pulposus* is a hydrated gel, a

semi-fluid mass, an incompressible sphere that exerts pressure in all directions. The *annulus fibrosus* consists of 15-25 concentric laminated layers of collagen lamellae tightly connected to each other in a circumferential form around the periphery of the disc. Each lamella consists of ground substance and collagen fibers. Within each lamella the collagen fibers are arranged in parallel, running at an average direction of 30° to the discs horizontal plane. In adjacent lamellae they run in opposite directions and are therefore oriented at 120° to each other. The *cartilaginous endplates* separate the nucleus and annulus from the vertebral bodies, they cover almost the entire surface of the adjacent vertebral bony endplates. The plates have a mean thickness of 0.6 mm.

Seven types of *ligaments* are distinguished in the lumbar spine. The *anterior longitudinal ligament* covers the anterior surfaces of the vertebral bodies and discs, attached strongly to the vertebral bone and weakly to the discs. The *posterior longitudinal ligament* covers the posterior aspects of the vertebral bodies and discs, attached strongly to the discs and weakly to the bone. The *ligamentum flavum*, the most elastic ligament of the spine connects the lower and upper ends of the internal surfaces of the adjacent laminae. The *intertransverse ligaments* connect the transverse processes by thin sheets of collagen fibers. The *interspinous ligaments* connect the opposing edges of spinous processes by collagen fibers, while the *supraspinous ligaments* connect the peaks of adjacent spinous processes by tendinous fibers. The *capsular ligaments* connect the circumferences of the joining articular facet joints, being perpendicular to the surface of the joints.

The *muscles* of the lumbar spine can be distinguished by their location around the spine. The *postvertebral muscles* can be divided to deep, intermediate and superficial categories. The *prevertebral muscles* are the abdominal muscles. The postvertebral deep muscles consist of short muscles that connect the adjacent spinous and transverse processes and laminae. The intermediate muscles are more diffused, arising from the transverse processes of each vertebra and attaching to the spinous process of the vertebra above. The superficial postvertebral muscles collectively are called the *erector spinae*. There are four *abdominal muscles*, three of them encircle the abdominal region, and the fourth is located anteriorly at the midline.

A *motion segment* or *functional spinal unit* (FSU) is the smallest part of the spine that represents all the main biomechanical features and characteristics of the whole spine. Thus the entire spinal column can be considered as a series of connecting motion segments. The motion segment is a three dimensional structure of six degree of statical/kinematical freedom, consisting of the two adjacent vertebrae with its posterior elements and facet joints, and the intervertebral disc between them, moreover the seven surrounding ligaments, without muscles.

3. Biomechanics of the lumbar spine and spine segments

The spinal column is the *main load bearing structure* of the human musculoskeletal system. It has three fundamental biomechanical functions: *to guarantee the load transfer* along the spinal column without instability; *to allow sufficient physiologic mobility* and flexibility; and *to protect the delicate spinal cord* from damaging forces and motions.

The lumbar spine is the most critical part of the spine in aspect of instability and injury since this part is the maximally loaded part of spine and this part has the maximal mobility at the same time, moreover, this part has the minimal stiffening support from the surrounding organs.

3.1 Loads acting on the lumbar spine

The spinal loads based on biomechanical studies are summarized by Dolan and Adams (2001). The loads acting on the spine can be physiologic and traumatic loads. The *physiologic loads* due to the common, normal activity of the spine have further classes: short-term loads (in flexion, extension), long-term loads (in sitting, standing), repeated or cyclic loads (in gait, walk), dynamic loads (in running, jumping). The *traumatic loads* generally occur suddenly, unexpectedly with great amplitude (impact, whiplash).

Each part of the body is subjected to *gravity load*, proportionally to its mass. The compressive gravity load increases towards the support of the body. This load can be multiplied in acceleration, during a fall, or other effects with acceleration or deceleration.

Muscle loads depend on the muscle activity. The muscles are active tissues, they can contract, and their ability of contraction is governed by the nervous system. The back and abdomen muscles stabilize the spine in upright standing; moreover, they prevent the spine from extreme movements. At the same time, the muscle contraction causes high compressive forces to the lumbar spine. Nachemson (1981) and Sato et al. (1999) classified the muscle forces in different body postures.

The *intra-abdominal pressure* decreases generally the spinal compression due to the abdominal muscle activity. Wide abdominal belts help to reduce the spinal compressive forces.

Ergonomic loads afflict mostly the lumbar spine. By lifting and holding weights the lumbar spine is subjected to high compressive load, depending on the horizontal distance of the load from the lumbar spine. Long-term vibration and cyclical effects may increase the compression in the lumbar spine leading to structural changes and fatigue effects in the tissue of discs and vertebrae.

Traumatic overload of the spine may cause damage in the discs and facet joints. Although muscles can save the spine from excessive injurious loads and movements, this protection works only if the neural system has time enough to activate the muscles.

3.2 Internal forces arising in the lumbar spine

The main internal force acting on the lumbar spine is the *compressive normal force* acting perpendicularly to the middle plane of the discs, causing the compression of the discs. It is accompanied by mainly sagittal and less lateral *shear forces* acting in the middle plane of the discs, causing the slope of the discs to each other. The moment components causing the forwards/backwards bending (flexion/extension) and the lateral bending of the spine are the sagittal and lateral *bending moments*, respectively; and the component that causes the spine to rotate about its long axis is the *torque or torsional moment*. The *tensile force* is also a normal force acting perpendicularly to the middle plane of the discs and causing the elongation of it. Although from physiologic loads there is no pure tensile force acting on the spine, since it acts

generally to a part of the discs only as a side effect of other internal forces, however, the aim of traction therapies is even to apply pure tensional force to the lumbar spine.

3.3 Mobility of the lumbar spine

The range of *spinal movements* can be measured both in vivo and in vitro. The spinal movement has six components: three deflections and three rotations. The physiologic movements are the flexion and extension in the sagittal plane, the lateral bending in the frontal plane and the rotation around the long axis of the spine. The spinal motions are generally characterized by three parameters: the *neutral zone* in which the spine shows no resistance, the *elastic zone* in which the spinal resistance works, and the *range of motion,* the sum of the two latter zones.

The mobility of the spine depends on several factors. It depends first of all on the state of the intervertebral discs: the geometry, the stiffness, the fluid content, the degeneration and aging of it. The lumbar region of the spine has greater mobility than the thoracic spine. The range of motion is influenced also by the state of ligaments, the articular facet joints and the posterior bony elements. Viscoelastic properties of discs and ligaments also have an effect on the mobility.

3.4 Biomechanics of the lumbar functional spinal units

The three-dimensional FSU has six force and six motion components that depend highly on the mechanical properties, stiffness or flexibility, load bearing capacity of each structural component of the motion segment, that all depend on the age and degeneration state of them.

Lumbar *vertebral bodies* resist most of the compressive force acting along the long axis of the spine. Most of this load must resisted by the dense network of trabeculae, and less by the cortical shell. The state of the cancellous bone is the main factor of compressive failure tolerance of vertebrae (McGill, 2000). Moreover, the cancellous bone of vertebrae acts as shock absorber of the spine in accidental injurious effects. The load bearing capacity of vertebrae depends on the geometry, mass, bone mineral density (BMD) and the bone architecture of the vertebra, which all are in correlation with aging sex and degeneration. Mosekilde (2000) demonstrated that age is the major determinant of vertebral bone strength, mass, and micro-architecture. The posterior elements of vertebrae have also important role in the load bearing capacity and mobility of segments. Facet joints work as typical contact structures, by limiting the spinal movements. They stabilize the lumbar spine in compression, and prevent excessive bending and translation between adjacent vertebrae, to protect the disc and the spinal cord.

The *intervertebral discs* provide the compressive force transfer between the two adjacent vertebrae, and at the same time they allow the intervertebral mobility and flexibility. The arrangement of the collagen fibers in the annulus fibrosus is optimal for absorbing the stresses generated by the hydrostatic compression state nucleus pulposus in axial loading of the disc, and they play an important role in restricting axial rotation of the spine. Axial compressive stiffness is higher in the outer and posterior regions than in the inner and anterior regions. Tensile stiffness is higher in the anterior and posterior part than in the

lateral and inner regions. Thus, the inner annulus near the nucleus seems to be the weakest area of annulus, and the outer posterior part the strongest region. In sustained loading the spine shows viscoelastic features. In quasi-static compression the disc creep is 5-7 times higher than the creep in the bony structures of the segment. Thus, the main factor of segment viscosity is the disc, mainly the disc annulus. The creep of the disc depends on the fluid content of it, mainly on the diurnal variation of it, namely on the fluid loss of daily activity and the overnight bed rest with fluid recovery.

The *ligaments* are *passive tissues* working against tension only. The primary action of the spinal ligaments lying posterior to the centre of sagittal plane rotation is to protect the spine by preventing excessive lumbar flexion. However, during this protection the ligaments may compress the discs by 100% or more. Indeed, the effectiveness of a ligament depends mainly on the moment arm through which it acts. The most elastic ligament, the ligamentum flavum being under pretension throughout all levels of flexion prevents any forms of buckling of spine. The interspinous and supraspinous ligaments may protect against excessive flexion. The capsular ligaments of facet joints restrict joint flexion and distraction of the facet surfaces of axial torsion.

The *muscles* being *active tissues* governed by the *neuromuscular control* are required to provide dynamic stability of the spine in the given activity and posture, and to provide mobility during physiologic activity, moreover to protect the spine during trauma in the post-injury phase. Two mechanical characteristics are necessary to provide these physiologic functions: the muscles must generate forces isometrically and by length change (contraction and elongation), and they must increase the stiffness of the spinal system.

The mechanical behaviour of the whole *functional spinal units* (FSU) depends on the physical properties of its components, mainly on the behaviour of the intervertebral disc, ligaments and articular facet joints. The average *load tolerance* of lumbar segments under quasi-static loading is about 5000 N for compression, 2800 N for tension, 150 N for shear and 20 Nm for axial rotation (Bader and Bouten, 2000). *Flexibility* of the FSU is the ability of the structure to deform under the applied load. Inversely, the *stiffness* is the ability to resist by force to a deformation. The stiffness of the spinal segments increases from cervical to lumbar regions for all loading cases. In lumbar region the stiffness is about 2000-2500 N/mm for compression, 800-1000N/mm for tension, 200-400 N/mm for lateral and 120-200 N/mm for anterior/posterior shear. The rotational stiffness is about 1.4-2.2 Nm/degree for flexion, 2.0-2.8 Nm/degree for extension, 1.8-2.0 Nm/degree for lateral bending and 5 Nm/degree for axial torsion (White and Panjabi, 1990; Bader and Bouten, 2000). The stiffness of the lumbar spine depends on the age and degeneration. In advanced degeneration the stiffness is higher. The stiffness is influenced by the viscous properties of the segments and the load history as well.

4. Degeneration of the lumbar spine and spine segments

The lumbar part is the most vulnerable section of the spine since both the compressive loads and the spinal mobility are maximal in this area. Consequently, the lumbar discs are mostly endangered by degenerations that influence the load bearing capacity of the segments. *Degeneration* means an injurious change in the function and structure of the disc, caused by *aging* or by *environmental effects*, like mechanical overloading (Adams et al., 2000).

Degeneration of FSU starts generally in the intervertebral discs. The first age-related changes of disc occur within the nucleus. Changes to any tissue property of the disc markedly alter the mechanics of load transfer and stability of the whole segment (Ferguson and Steffen, 2003). The mechanical properties of the segment depend also on the state of the bony structures, first of all on the trabecular structure of the internal spongy bone of vertebrae. The osteoporotic changes may also decrease the load bearing capacity of FSU.

Long-term age-related degeneration of the discs is manifested in the loss of hydration, a drying and stiffening procedure in the texture of mainly the nucleus (McNally and Adams 1992; Adams et al., 2002; Cassinelli and Kang, 2000). The functional consequences of aging are that the nucleus becomes dry, fibrous and stiff. The volume of nucleus and the region of hydrostatic pressure of it decrease, consequently, the compressive load-bearing of the disc passes to the annulus. The age-related changes of disc can be accompanied by the appearance of buckling, lesions, tears, fiber break in the annulus or disruption in the endplates, collapse of osteoporotic vertebral cancellous bone. Since the annulus becomes weaker with aging, so the overloading of it can lead to the inward buckling of the internal annulus, or to circumferential or radial tears, fiber break in the annulus, disc prolapse or herniation, or to large radial bulging of the external annulus, reduction of the disc height, or moreover, to endplate damages (Natarajan et al., 2004). The main cause of all these problems is that while the healthy disc has a hydrostatic nucleus, during aging, it becomes fibrous being no longer as a pressurized fluid. Several recent studies concluded that light degeneration of young discs leaded to instability of lumbar spine, while the stability restored with further aging (Adams et al., 2002).

Sudden accidental, often unexpected traumatic degeneration or damage of overload may yield the sudden loss of hydrostatic compression in nucleus, accompanied or due to some other failures mentioned above. In these cases the material of nucleus remains changeless, depending on the actual aging state in which the accidental effect happened. For this reason, sudden traumatic degenerations may be also dangerous in younger age.

Experimental analyses of spinal degenerations are very difficult, sometimes impossible. However, by means of numerical simulation, the effect of the main mechanical factors of degenerations can be analyzed.

5. Finite element modeling of the lumbar spine

Finite element modeling of any structure consists of five main steps: geometrical, material, element type and load modeling, and finally, validating the complete model.

5.1 Geometrical modeling of the lumbar spine segments

Geometrical modeling of the FSU must follow the anatomy of the segment. Beside the topology, additional data such as volume density, surface texture, etc. are needed. Different methods of medical image analyses can be used, like scanners, computer tomography, or magnetic resonance imaging methods.

In geometrical modeling the *vertebral body*, its cortical shell, cancellous core, posterior bony elements and the bony endplates are generally distinguished. For the width of the

cylindrical vertebral body, 40-45 mm, for the depth 30-35 mm, and for the height 25-29 mm is generally used. For the thickness of the vertebral cortical wall about 1-1.5 mm, and for the thickness of the cartilaginous endplates 0.5-1 mm, and for the thickness of the cartilage layer of facet joint 0.2 mm, for the area about 1.6 cm² are generally used.

In geometrical modeling the *intervertebral disc*, for the height of it about 8-12 mm are generally used, depending on the sex and body height of the subject. In the disc model, the nucleus, the annulus ground substance, the annulus fibers and the cartilaginous endplates are generally distinguished. For the volumetric relation between annulus and nucleus, ratio 3:7 is generally used for the lumbar part L1-S1, and for the area ratio of nucleus 30-50% of the total disc area in cross section is generally used. The sagittal diameter length of the lumbar disc is about 36 mm, the lateral length is about 44 mm. For the orientation of annulus fibers to the mid cross-sectional area of the disc about 30° is used.

As for the cross sectional area of the *ligaments*, for the anterior longitudinal ligaments about 30-70 mm², for the posterior longitudinal ligaments about 10-20 mm², for the ligamentum flavum 40-100 mm², for the capsular ligaments about 30-60 mm², for the intertransverse ligaments 2-10 mm², for the interspinous ligaments 30-40 mm², for the supraspinous ligaments 25-40 mm² are generally used.

In modeling the *degenerated segments*, the height of both the vertebrae and the disc is reduced. Volume reduction of the nucleus during aging is also considered.

5.2 Material modeling of the lumbar spine segments

Since FSU is a highly heterogeneous compound structure, the material modeling must be related to the components of it. First the material models of the healthy components are considered.

The detailed data of the material modeling based on the international literature can be studied in Kurutz (2010).

5.2.1 Material models of the healthy lumbar segments

The material models and constants of the components of FSU were generally obtained by experimental mechanical tests of certain specimens obtained from the given component.

The high strength *vertebral cortical shell* is generally considered linear elastic isotropic or transversely isotropic, orthotropic material. In linear elastic isotropic case its Young modulus is considered about 5000-12000 MPa with the Poisson ratio about nu=0.2-0.3. In linear elastic, transversely isotropic case these data are E=12000-22000 MPa and G=3000-5000 MPa with nu=0.2-0.4 in the compressive direction, and E=8000-12000 MPa and G=3000-5000 MPa with nu=0.4-0.5 perpendicularly.

The vertebral *cancellous bone* is modeled generally also as linear elastic isotropic or transversely isotropic, or orthotropic material. In linear elastic isotropic case its Young modulus is considered about 10-500 MPa with the Poisson ratio about nu=0.2-0.3. In linear elastic, transversely isotropic case these data are E=200-250 MPa and G=50-80 MPa with nu=0.3-0.35 in the compressive direction, and E=100-150 MPa and G=50-80 MPa with nu=0.3-0.45 perpendicularly.

The high strength *bony endplate* of vertebrae and the lower strenght *cartiliginous endplate* of disc can hardly be distinguished when specifying material properties. Both bony and cartilaginous endplates are considered generally linear elastic isotropic material, with E=100-12000 MPa and nu=0.3-0.4, and E=20-25 MPa with nu=0.4, respectively.

The *posterior bony elements* are considered linear elastic isotropic material, generally by the same Young's modulus E=2500-3000 MPa and Poisson's coefficient nu=0.2-0.25.

The *articular facet joints* are considered as unilateral friction or frictionless connections with an initial gap of generally 0.5-1 mm.

Disc nucleus pulposus is the most important element in the compressive stiffness of the disc: the hydrostatic compression in it guarantees the stability of the whole disc and segment. The healthy young nucleus is generally modeled as an incompressible fluid-like material. In the case of fluid like linear elastic isotropic solid generally the material moduli E=1-4 MPa with nu=0.49-0.499 are considered. Several authors model the nucleus as incompressible fluid, quasi incompressible fluid, hyperelastic neo-Hookean, or Mooney-Rivlin type material, moreover, poroelastic or viscoelastic or osmoviscoelastic solid with the concerning material data (Kurutz, 2010).

Disc annulus fibrosus is a typical composite-like material with a ground substance of many layers and fiber reinforcements. Material moduli of the ground substance are considered as E=2-10 MPa with nu=0.4-0.45, and of the fibers E=300-500 MPa depending of the radial position, with nu=0.3.

Numerical modeling of *ligaments*, as typical exponentially stiffening soft tissues is not a simple task. Generally, the seven ligaments are incorporated to the FE models as tension only elements. In contrast to its strong nonlinear behaviour (White and Panjabi, 1990), most of the reported FEM studies have adopted linear or bilinear elastic models.

5.2.2 Material models of the degenerated lumbar segments

Aging type degeneration starts generally in the nucleus. A healthy young fluid-like nucleus is in a hydrostatic compression state. During aging, the nucleus loses its incompressibility and becomes even stiffer and stiffer, changing from fluid to solid material. This kind of nucleus degeneration can be modeled by decreasing Poisson's ratio with increasing Young's modulus. This behavior is generally accompanied by the stiffening process of the disc as a whole and by the volume reduction of the nucleus and volume extension of the annulus, furthermore, height reduction of the disc. Moreover, at the same time, annulus tears or internal annulus buckling, or break of the annular fibers, damage and crack or rupture of endplates, osteoporotic defects of vertebral cancellous bone can happen. Consequently, modeling age-related degeneration of FSU is a compound task; it must be done in progress, relating to a lifelong process.

In contrast to the age-related degeneration, in *sudden, often unexpected injurious degeneration* the nucleus may lose its incompressibility without any stiffening and volume change process. In this case the nucleus may quasi burst out and the hydrostatic compression may suddenly stop in it. This kind of nucleus degeneration can be modeled by suddenly decreasing Poisson's ratio with unchanged Young's modulus of nucleus (Kurutz and

Oroszváry, 2010). This behaviour is generally caused or accompanied by the tear or buckling of the internal annulus, break of the annular fibers, fracture of endplates, or collapse of vertebral cancellous bone, depending on the age in which the sudden accidental event happens. Namely, accidental failures can happen in a young disc, as well, or in any age and aging degeneration phases. These effects can be modeled by sudden damage of tissues of the concerning components of the segment. In contrast to the long term aging degeneration, these kinds of damage instability occurs suddenly, generally due to a mechanical overloading (Acaraglou et al., 1995).

The material modeling of segment degeneration can be studied in Kurutz (2010).

5.3 Element type modeling of the lumbar segments

The cancellous core and the posterior bony elements of *vertebrae* can be modeled as 3D solid continuum elements, as isoparametric 8-node hexahedral elements, or as 20- or 27-noded brick elements, moreover, as 10-noded tetrahedral elements. The cortical shell and the endplates can be modeled as thin shell elements, like 4-node shell elements. Quasi-rigid beam elements can connect the posterior vertebra with the medial transverse processes (pedicles) and from the medial transverse processes to the medial spinous process (lamina). Beam elements can also be used to represent the transverse and spinous processes. The bony surface of the facet joints can be represented by shell elements where beam elements link these facets to the lamina, simulating the inferior and superior articular processes. The facet joints can be modeled as 3D 8-noded surface-to-surface contact elements.

The *disc* annulus ground substance is generally modeled as 3D continuum elements. The collagen fibers can be modeled as truss elements or as reinforced bar (rebar) type elements embedded in 3D solid elements. The nucleus pulposus can be modeled as hydrostatic fluid volume elements.

The anterior and posterior longitudinal *ligament*s can be modeled as thin shell elements, or, the ligaments can be modeled as 2-noded axial elements, that is, tension only linear or nonlinear truss or cable or spring elements.

5.4 Load models of the lumbar spine

Loads on lumbar spinal motion segments depend on the aims of the analysis. The segment is generally supported rigidly along the inferior endplate of the lower vertebra, thus, the loads are generally applied on the superior endplate of the upper vertebra.

The loads can be applied as static or dynamic or cyclic loads. Constant static loads or incrementally changing quasi-static loads are generally applied in lumbar spine analyses. In load history analyses the basic loading types are the force or displacement loads, in a load or displacement controlled device.

For different loading, pre-compression is also applied for modeling the upper body weight as 700-1000 N, simulating the intervertebral pressure of standing position and additional compressive forces can be applied to the suitable areas of the endplates to simulate severe motions: 2000 N for lifting a load with straight legs in full flexion; 1000 N for full extension; 1300 N for full lateral bending. For flexion and extension and for axial torsion generally 10-15 Nm is applied.

The loading system of numerical simulation applied by several authors can be studied in Kurutz (2010).

The compressive strength of the lumbar spine varies between 2 kN and 14 kN, depending on the sex, age and bodymass (Adams et al, 2002). For injurious accidental degeneration load for compression about 5 kN can be considered for young, and about 3 kN for old subjects. The lumbar facet joints can resist about 2 kN for shear before fracture occurs. For torsion, damage is initiated when the applied torque rises to about 10-30 Nm. A combination of full backwards bending and 1 kN of compressive load can cause damage in the relating facet joint. In forward bending, injury can occur when the bending moment rises to 50-80 Nm.

5.5 Validation of the finite element models

By using FE models in a numerical simulation, the results should be trustworthy. For this reason, the models to be applied must be checked. Correlation between FE and experimental results can lead to use the FE model predictions with confidence.

In numerical simulations of biomechanics, for FE prediction accuracy assessment, a gold standard can be the experimental validation of numerical results. This enables the analyst to improve the quality and reliability of the FE model and the modeling methodology. If there is very poor agreement between the analytical and experimental data, by using certain numerical techniques for model updating allow the user to create improved models which represent reality much better than the original ones.

Kurutz and Oroszváry (2010) validated the lumbar segment model for both compression and tension and for both healthy and degenerated disc. Distribution of vertical compressive stresses of healthy and degenerated discs in the mid-sagittal horizontal section of the disc was compared with the experimental results of Adams et al. (1996, 2002), obtained by stress profilometry. In axial tension, the calculated disc elongations were compared with the in vivo measured elongations of Kurutz et al. (2003) and Kurutz (2006a) for healthy and degenerated segments in weightbath hydrotraction treatment (Kurutz and Bender, 2010).

6. Finite element simulation of the behaviour of healthy and degenerated lumbar spine and underwater spinal traction therapy

Finite element analyses are able to simulate processes in progress that are impossible to measure experimentally, like spinal degeneration processes. 3D FE simulations of long-term age-related and sudden accidental degeneration processes of human lumbar spinal segments are presented to analyze the compression-related degeneration processes, moreover, to analyze the efficiency of the so-called weightbath hydrotraction treatment.

A 3D geometrical model of a typical lumbar segment L4-5 was created (Fig. 1a). The geometrical data of the segment were obtained by the anatomical measures of a typical lumbar segment (Denoziere, 2004). Cortical and cancellous bones of vertebrae were separately modeled, including posterior bony elements. The thickness of vertebral cortical walls and endplates were 0.35 and 0.5 mm, respectively. For this simple model, we kept the disc height constant by applying 10 mm height. Annulus fibrous consisted of ground substance and elastic fibers (Fig. 1b). Annulus matrix was divided to internal and external

ring; with three layers of annulus fibers of 0.1 mm² cross section. The geometry and orientation of facet joints were chosen according to Panjabi et al. (1993).

FE mesh was created in three steps (Fig. 1c). First the geometrical model of FSU was created by using Pro/Engineer code; then the FE mesh was generated by ANSYS Workbench; finally, the several components were integrated to the FE model by ANSYS Classic.
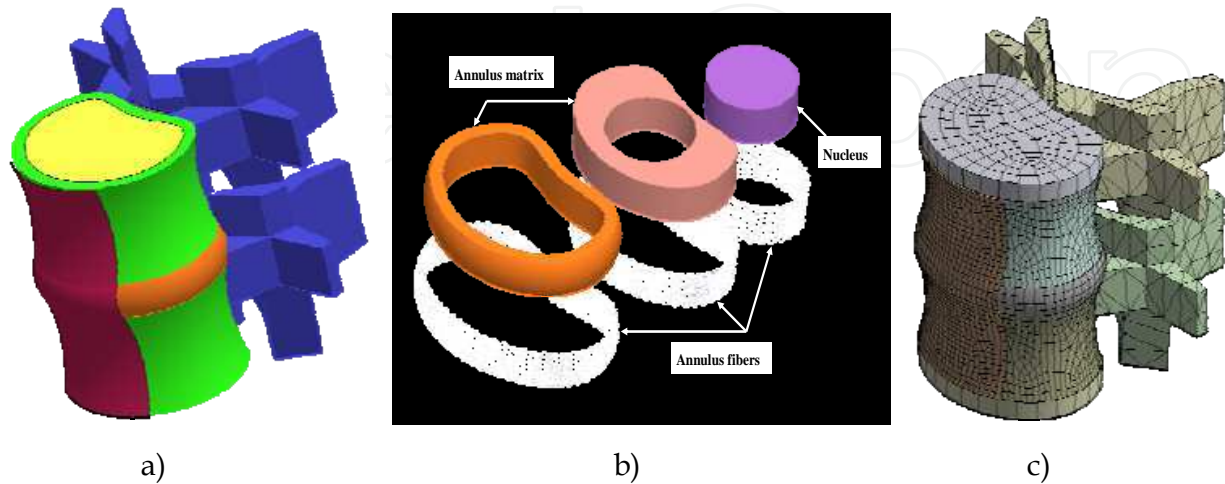

| a) | b) | c) |

Fig. 1. The geometrical model of a) the segment and b) the intervertebral disc and c) the finite element mesh of the segment

The material moduli of the healthy segment (Table 1) were obtained from the literature (Rohlmann et al., 2006; Goel et al., 1995; Denoziere, 2004; Denoziere and Ku, 2006; Cheung et al., 2003; Antosik and Awrejcewicz, 1999; Noailly et al., 2007; Williams et al., 2007; Shirazi-Adl et al, 1984, 1986; Shirazi-Adl, 1989; Lavaste et al., 1992; Zander et al., 2004). For the bony elements and endplates we considered linear elastic isotropic materials for both tension and compression. Annulus ground substance and nucleus were considered linear elastic for both compression and tension. For the fluid-like healthy nucleus and for the annulus matrix also linear elastic material was considered.

Components of FSU	Young's mod [MPa]	Poisson's ratio
Vertebral cortical bone	12000	0,3
Vertebral cancellous bone	150	0,3
Posterior elements, facet	3500	0,3
Endplate	100	0,4
Annulus ground substance	4	0,45
Annulus fibers	500/400/300*	-
Nucleus	1	0,499
Anterior longitud. ligament	8**	0,35
Posterior longitud. ligament	10**	0,35
Other ligaments	5**	0,35

*external/middle/internal fibers, tension   **tension only

Table 1. Material moduli of the components of healthy segment

Collagen fibers of the annulus were considered as bilinear elastic isotropic tension-only material. To simulate the radial variation of collagen in the fibers, the stiffness of them was increased outwards. All seven ligaments were integrated in the model with bilinear elastic tension-only material.

For our numerical experiments, the basic data of Table 1 were modified.

6.1 Finite element simulation of age-related degeneration processes of lumbar spine

Age-related degeneration starts generally in the nucleus. A healthy young nucleus is in hydrostatic compression state. During aging, the nucleus loses its incompressibility by changing gradually from fluid-like to solid material. This kind of nucleus degeneration was modeled by decreasing Poisson's ratio with increasing Young's modulus. This behavior is generally accompanied by the hardening process of the disc as a whole and by tears, buckling or fiber break of the annulus, and damage of endplates or vertebral cancellous bone. The data of five grades of normal aging degeneration process from healthy to fully degenerated case are seen in Table 2, by gradually decreasing Poisson's ratio with gradually increasing Young's modulus of nucleus, accompanied by aging of other tissues of FSU.

Grades of age-related degeneration* (Young's mod/Poisson's ratio)	grade 1 (healthy)	grade 2	grade 3	grade 4	grade 5 (fully deg.)
nucleus	1/0.499	3/0.45	9/0.4	27/0.35	81/0.3
annulus ground substance	4/0.45	4.5/0.45	5/0.45	5.5/0.45	6/0.45
cancellous bone	150/0.3	125/0.3	100/0.3	75/0.3	50/0.3
endplate	100/0.4	80/0.4	60/0.4	40/0.4	20/0.4

* Bony elements and annulus fibers are seen in Table 1

Table 2. Modeling of age-related degeneration process: material moduli of components of segments from healthy (1) to fully degenerated (5) phases

Simulating aging degeneration processes, 1000 N axial compression load was applied, by considering that the lumbar compression load is about 60% of the total body weight, completed by the muscle forces being nearly the same (Nachemson, 1981; Sato et al., 1999).

The compression load was distributed along the superior and inferior surface of the upper and lower vertebra of FSU, by applying rigid load distributor plates at both surfaces.

Figure 2 illustrates the maximum stress rearrange in the mid-sagittal section of the disc during the degeneration process. While in a healthy disc in Fig. 2a, due to the hydrostatic compression stress state, the maximum compressive stresses occur in the middle of nucleus, in a fully degenerated disc in Fig. 2b, due to the lost hydrostatic compression, the maximum compressive stresses move outwards to the edge of nucleus, towards the annulus ring.

Figure 3a shows the change of mid-sagittal vertical compressive stresses for aging degeneration models of Table 2, in the middle and border of nucleus and in the internal and external nucleus, for 1000 N axial compressive load. The vertical stresses in the center and border of nucleus first decreased and later increased with aging, yielding stress minimum in the nucleus in mildly degenerated state. In the internal annulus monotonous stress decrease

was observed, demonstrating the possible internal annulus buckling. In the external annulus the stresses slightly changed.
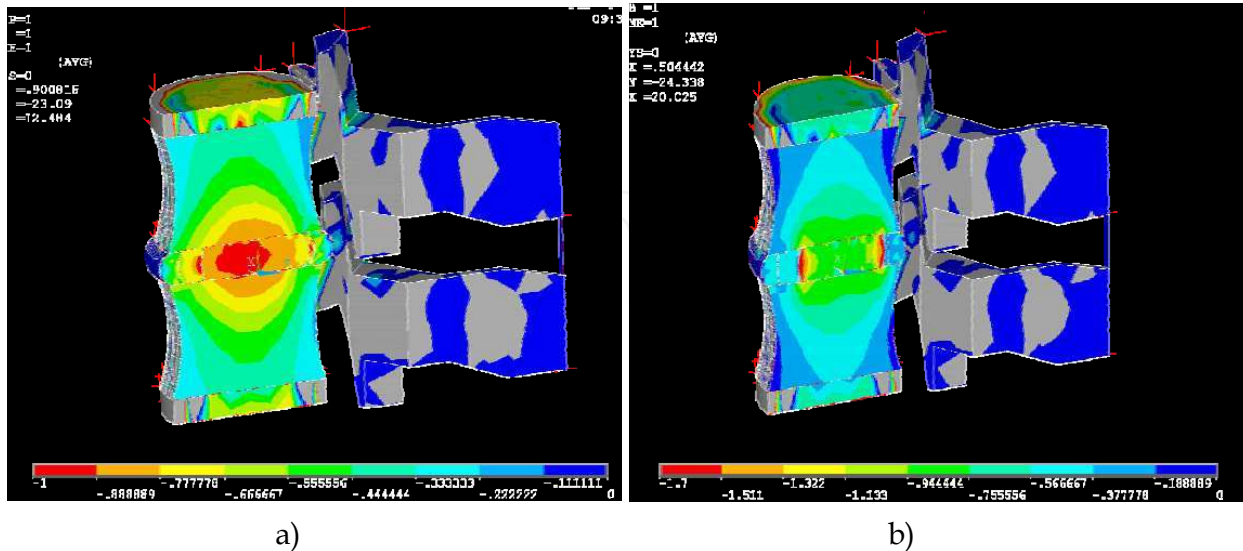

a)   b)

Fig. 2. Mid-sagittal vertical compressive stresses for a) healthy and b) fully degenerated disc
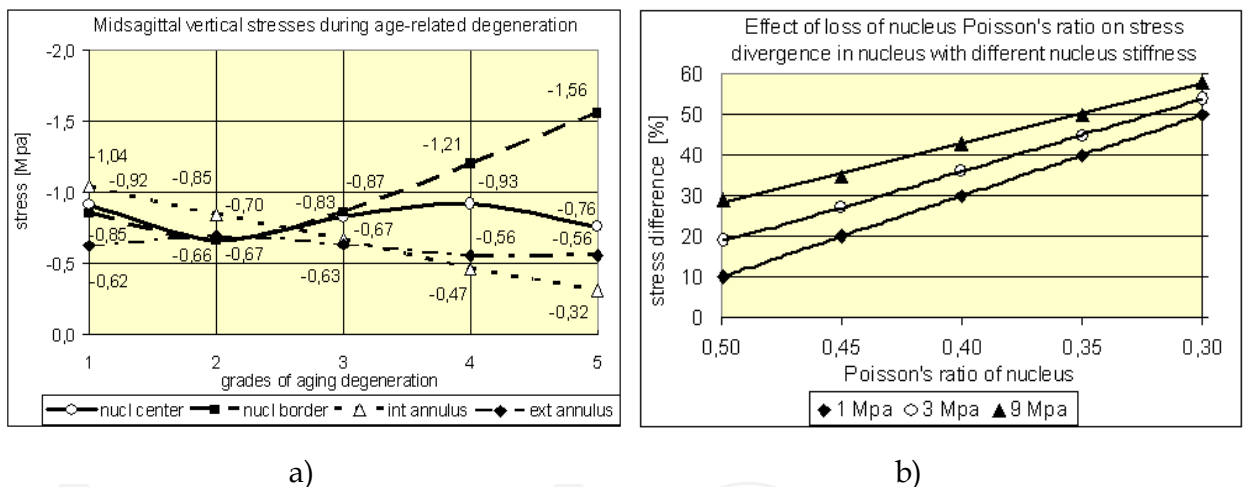

a)   b)

Fig. 3. a) Mid-sagittal vertical compressive stresses in disc components during aging degeneration and b) stress divergence in nucleus center during the loss of hydrostatic compression state in nucleus (Kurutz and Oroszváry, 2010).

In degenerated disc the pressure in the nucleus is not hydrostatic any more, being non-uniform and direction-dependent. In Fig. 3b the stress divergence is seen in the nucleus center between vertical and horizontal stresses, increasing rapidly and quasi linearly with the loss of hydrostatic compression in the nucleus. The initial stress divergence between vertical and horizontal stresses in hydrostatic state at nu=0.499 for the fluid-like nucleus of E=1 MPa was 8-10%, and naturally, for harder nucleus it was higher. By applying more fluid-like material for nucleus (E=0.1 MPa), the initial hydrostatic stress divergence could be decreased to 1-2%.

Fig. 4a illustrates the disc shortening with aging, demonstrating that the maximum disc deformability occurred in mild degeneration. Similar behaviour was observed for the

maximum tensile forces in the outermost posterolateral annulus fibers in Fig 4b, that is, the maximum fiber forces belonged also to the mildly degenerated state. Fig. 5a and 5b illustrate the tensile forces in healthy and fully degenerated annulus fibers, respectively.
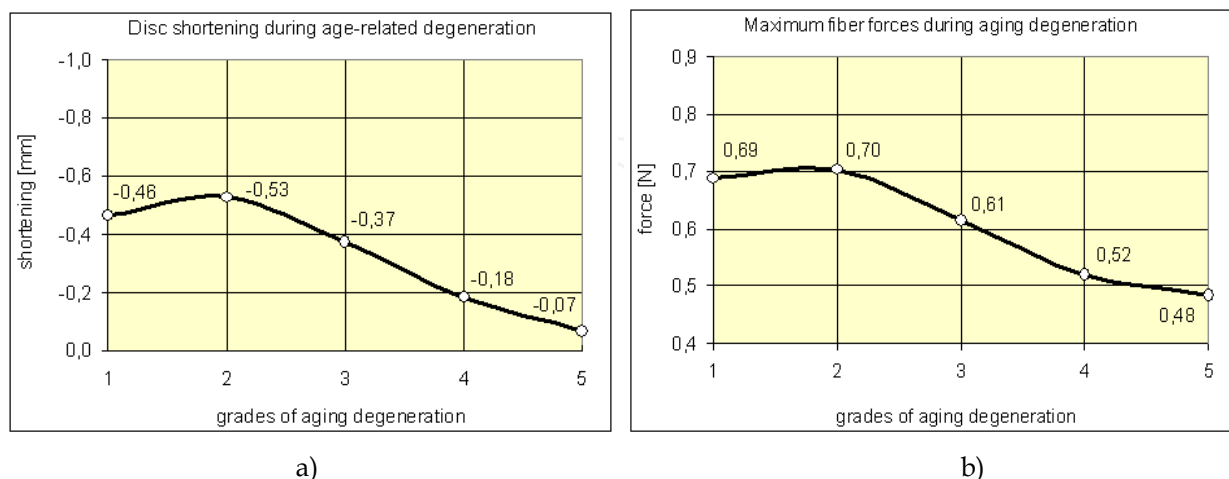

Fig. 4. a) Height loss of disc and b) maximum fiber forces during aging degeneration (Kurutz and Oroszváry, 2010)
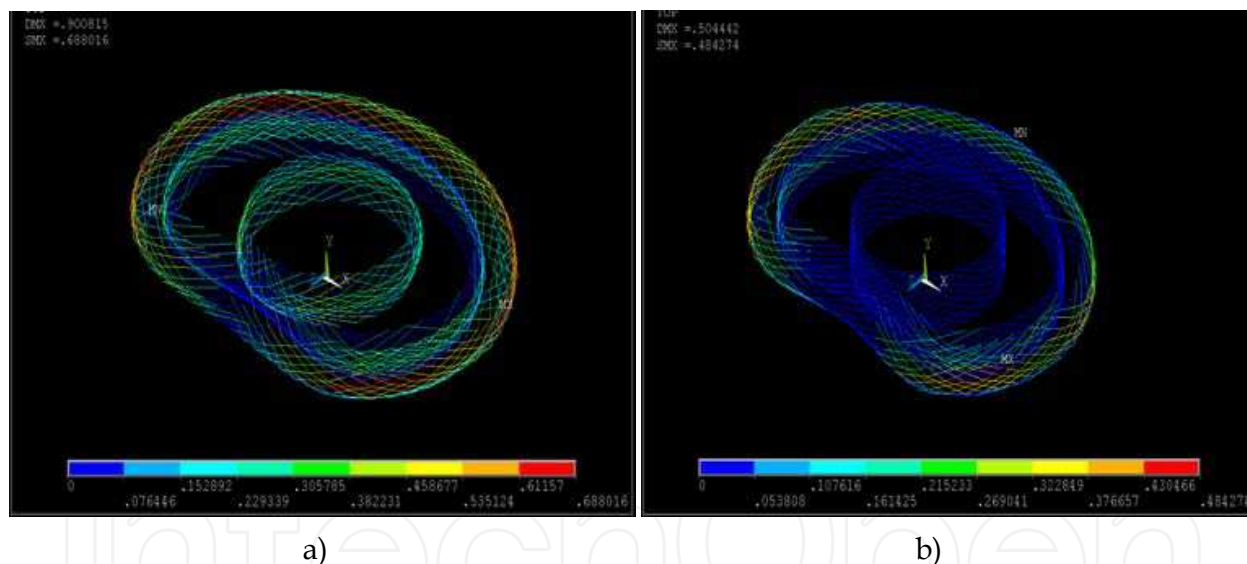

Fig. 5. Annulus fiber forces for a) healthy and b) fully degenerated case

Fig. 6a illustrate the change of posterior, anterior and lateral disc bulging during aging degeneration process, demonstrating that the bulging deformability is maximum in young age or mild degeneration, and it decreases with aging. Fig. 6b shows the change of the mean vertical compressive stiffness of disc components during the aging degeneration process. The minimum of each stiffness function belonged to the mildly degenerated state.

The stiffness of the whole disc depends mainly on the stiffness of the nucleus. In the first period of aging, the dominant effect is the loss of incompressibility of nucleus when the other disc components are considerable soft. This yields that the stresses and the vertical load transfer through the nucleus is minimum (Fig. 3a) and the deformability of disc is maximum in young age (Fig. 4a) leading to the minimum vertical compressive stiffness of

discs and the risk of instability of FSUs in mildly degenerated state (Fig. 6b.) Consequently, the lumbar segments are most vulnerable in young age, and the segmental stability increases with further aging and degeneration.
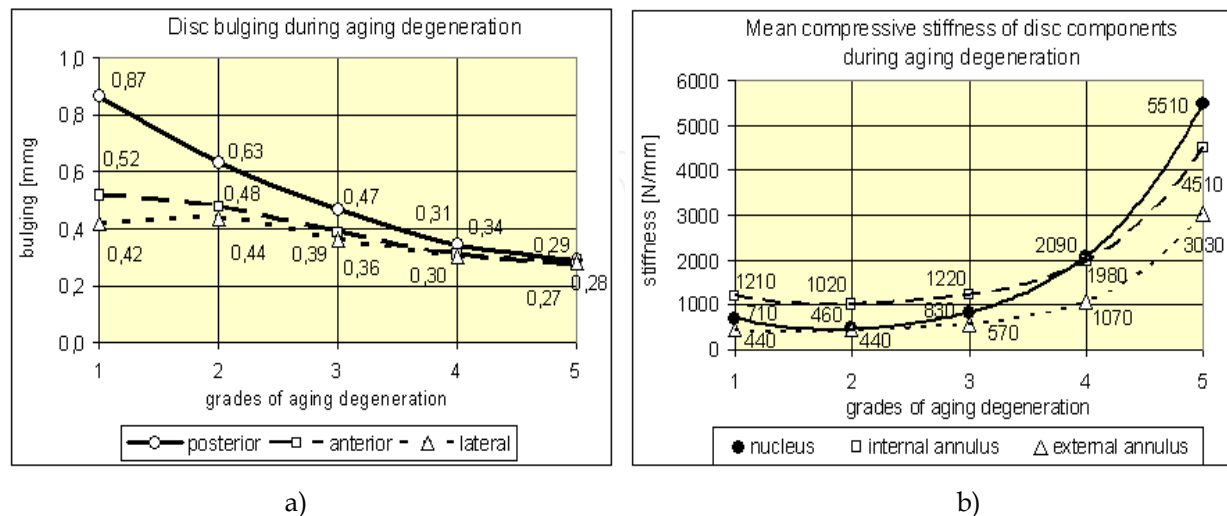

a)   b)

Fig. 6. a) Posterior, anterior and lateral disc bulging and b) mean compressive stiffness of disc components during aging degeneration (Kurutz and Oroszváry, 2010).

6.2 Finite element simulation of sudden degeneration processes of lumbar spine

In contrast to the age-related degeneration process that lasts during a lifelong time, the sudden degeneration has very short, sometimes unexpected, instant processes. For modeling sudden degeneration accompanied by other damaging phenomena, the data of the concerning tissues were modified in Table 1 and Table 2, depending on the actual aging degeneration phase in which the sudden accidental degeneration happened, considering also five phases of accidental degeneration process.

For example, data in Table 3 show the model of sudden degeneration in young age with annulus fiber breaks and tears. In this case the sudden degeneration happened in the first aging degeneration phase of Table 2, when the sudden loss of hydrostatic compression was modeled by rapid immediate decrease of Poisson ratio of nucleus with changeless Young's modulus of it. Annulus tears and fiber breaks were modeled by weakened annulus matrix and fibers, respectively, seen also in Table 3.

Phases of sudden degeneration* (Young's mod/Poisson's ratio)	grade 1	grade 2	grade 3	grade 4	grade 5
nucleus	1/0.499	1/0.45	1/0.40	1/0.35	1/0.3
annulus ground substance	4/0.45	3.5/0.45	3/0.45	2.5/0.45	2/0.45
annulus fibers	500/400/300	375/300/225	250/200/150	125/100/75	5/4/3

* Bony elements are seen in Table 1

Table 3. Modeling of sudden degeneration process with annulus tears and fiber break in young age: modified material moduli of components of segments

Simulating sudden accidental degeneration processes, the 1000 N axial compression load was completed by an unexpected sudden overload of 1000 N, thus, 2000 N axial compression load was applied.

Fig. 7a shows the sudden change of the mid-sagittal vertical compressive stresses in disc components, Fig. 7b illustrates the mid-sagittal central, posterior and anterior disc shortening during the sudden degeneration process in young age with annulus tears and fiber break (Table 3). The mean stress decreased strongly in the nucleus (by 70%), and moderately in the internal annulus (by 25%), while slightly increased in the external annulus (by 8-10%). Disc shortening radically increased during the process, finally by about 200-230%.

a)   b)
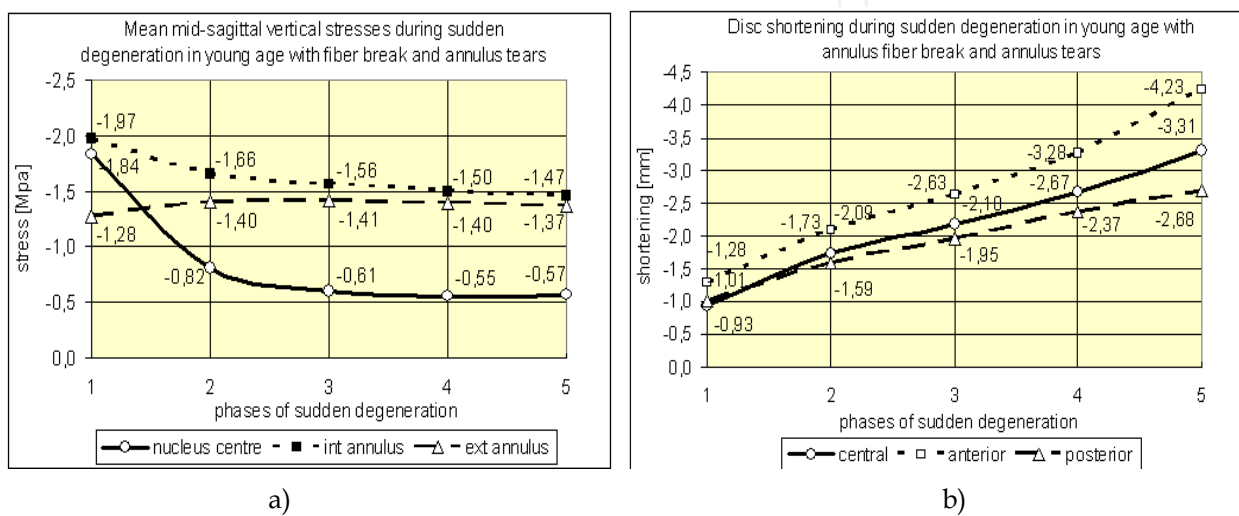
Fig. 7. a) Mid-sagittal vertical compressive stresses in disc components and b) disc shortening during sudden degeneration process

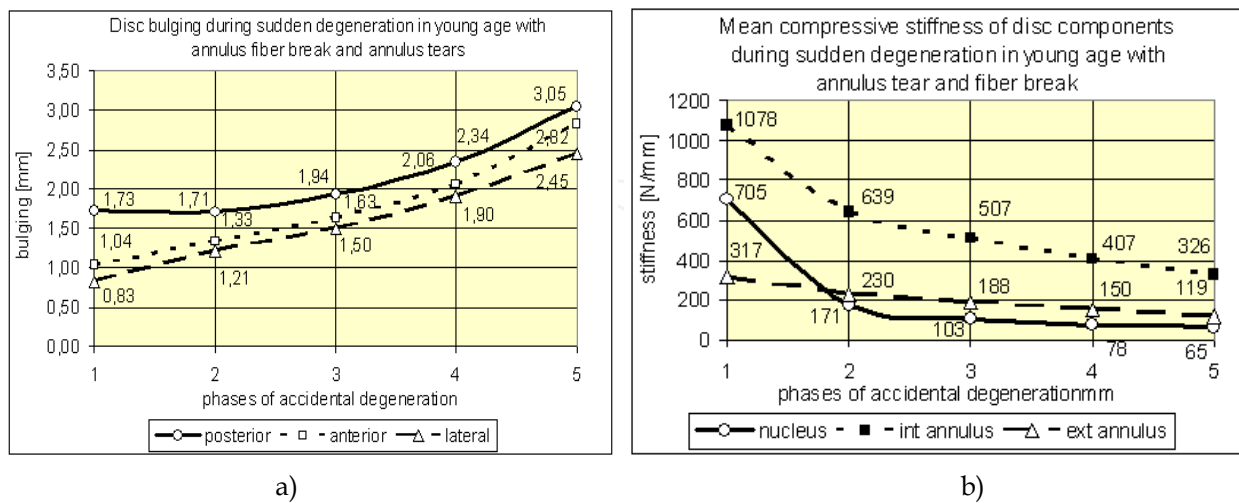a)   b)

Fig. 8. a) Posterior, anterior and lateral disc bulging and b) mean compressive stiffness of disc components during sudden degeneration process

Fig. 8a shows the sudden mid-sagittal anterior, posterior and lateral disc bulging. In Fig. 8b the mean compressive stiffness of disc components during the sudden degeneration process

are illustrated. Disc bulging radically increased in all directions (by 80-200%) due to the fiber breaks with radically decreasing maximum fiber forces from 1.38 N to 0.06 N. Significant stiffness loss was observed for the disc components (nucleus 91%, internal annulus 70%, external annulus 62%). The stiffness loss of the whole disc was 76%.

During sudden degeneration process the vertical compressive load transfer moves from inside to outside, from the nucleus to the external annulus during the progress of degeneration. In the case of internal annulus buckling, the sudden overload of the external annulus may lead to annulus tears and injury. In the case of fiber break and annulus tears, the internal annulus is overloaded.

In contrast to age-related degeneration processes where the disc deformability (shortening, bulging) decreases during aging, in sudden degeneration processes the deformability increases strongly that may lead to injury and pain mainly in younger age. Also in contrast to age-related degeneration processes where the vertical compressive stiffness of discs increases during aging, in sudden degeneration processes it decreases significantly leading to segmental instability and injury. In agreement with the literature we have found by numerical simulation of age-related degeneration that the young and mildly degenerated segments had the smallest stiffness and later the stiffness increased rapidly (Adams et al., 2002; Rohlmann et al., 2006; Schmidt et al., 2006, 2007). Similarly to the age-related degeneration, accidental degeneration may be the most dangerous in young age, due to the sudden stiffness loss starting at the smallest stiffness level, consequently, accidental disc shortening and bulging may cause sudden injury and low back pain in young age again.

6.3 Finite element simulation of weightbath hydrotraction treatment of lumbar spine

Kurutz and Oroszváry (2010) analyzed by FE simulation the stretching effect of a special underwater traction treatment applied for treating degenerative diseases of the lumbar spine, when the patients are suspended cervically in vertical position in the water, supported on a cervical collar alone, loaded by extra lead weights on the ankles.

The biomechanics of WHT has been reported first by Bene and Kurutz (1993). Elongations of lumbar segments during WHT have been measured in vivo by Kurutz et al. (2003). The clinical impacts of WHT have been analyzed by Oláh et al. (2008). The complex description of WHT has been given by Kurutz and Bender (2010) with its application, biomechanics and clinical effects. This numerical study aims to determine the disc elongation, bulging contraction, stress and fiber relaxation effects of WHT during age-related degeneration.

In this underwater cervical suspension, the traction load consists of two parts: (1) the removal of the compressive preload of body weight and muscle forces in water, named *indirect traction load*; and (2) the tensile force of buoyancy with the applied extra lead loads, named *direct traction load*. Based on mechanical calculations, for the standard body weight of 700 N, and the applied extra lead weights 40 N, the indirect and direct traction loads yields 840 N and 50 N, respectively. Thus, for the numerical analysis of WHT we applied 840 *N* indirect and 50 N direct traction loads.

In the finite element analysis of WHT the above detailed material, geometric and finite element model has been used. Annulus ground substance and nucleus were considered linear elastic in compression, and bilinear elastic in traction. Thus, for the five grades of age-

related degeneration process, in the indirect phase of traction, the compressive material moduli were used, seen in Table 2; while for the direct phase of traction, special tensile Young's moduli were applied, obtained by parameter identification (Kurutz and Tornyos, 2004), seen in Table 4. For healthy nucleus we applied fluid-like incompressible material both for tension and compression.

Grades of age-related degeneration for direct traction* (Young's mod/Poisson's ratio)	grade 1 (healthy)	grade 2	grade 3	grade 4	grade 5 (fully deg.)
nucleus	0.4/0.499	1.0/0.45	1.6/0.4	2.2/0.35	2.8/0.3
annulus ground substance	0.4/0.45	1.0/0.45	1.6/0.45	2.2/0.45	2.8/0.45
cancellous bone	150/0.3	125/0.3	100/0.3	75/0.3	50/0.3
endplate	100/0.4	80/0.4	60/0.4	40/0.4	20/0.4

* Bony elements and annulus fibers are seen in Table 1

Table 4. Modeling of age-related degeneration process for direct traction in WHT: material moduli of components of segments from healthy (1) to fully degenerated (5) phases

The unloading effect of WHT in its instant elastic phase is illustrated in Fig. 9 and 10 in terms of aging degeneration. The term 'unloading' is relative: it is related to the compressed state of segments just before the treatment. Due to the bilinear behaviour of the disc during hydrotraction, the results of deformation and stress unloading are distinguished: caused by indirect and direct traction loads.

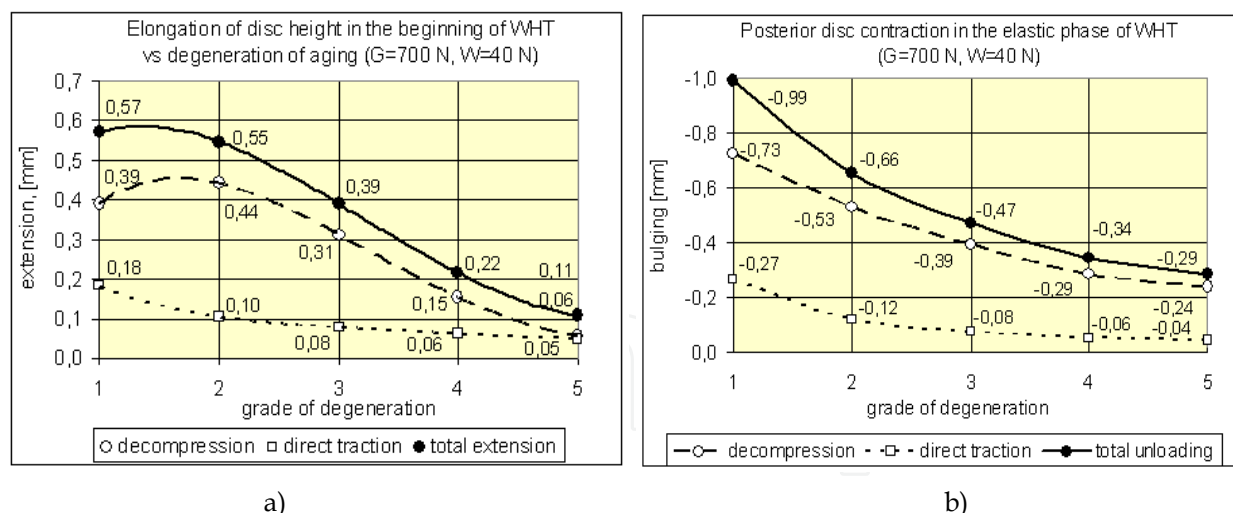a)   b)

Fig. 9. Unloading effect of WHT on a) disc compression and b) posterior disc bulging (Kurutz and Oroszváry, 2010).

In Fig. 9a the relative elongations of discs are seen compared with their compressed state before the treatment. These initial elastic elongations will be quasi doubled in the creeping phase of WHT (Kurutz, 2006b). The ratio of direct traction extensions versus total extensions is 32%, 19%, 20%, 28% and 47% for degeneration grades 1 to 5, respectively. The ratios of direct/indirect extensions are: 47%, 24%, 25%, 39% and 89%. The minimum ratio belongs to

the mild degeneration and increases rapidly with advanced degeneration and aging. The maximum ratio belongs to the fully degenerated cases.

The unloading of posterior bulging, namely, the relative disc contractions can be seen in Fig. 9b. The ratio of direct/total traction contractions decreases monotonously from 27% to 15% for posterior bulging for degeneration grades 1 to 5. The ratio of direct/indirect contractions changes from 37% to 18% in posterior bulging. The minimum ratio belongs to the fully degenerated case.

Fig. 10a and 10b show the vertical stress relaxation in the centre of nucleus and in the annulus external ring. The ratio of direct/total and direct/indirect stress unloading is equally small, 7-8% in healthy and 2-4% in fully degenerated cases. Thus, in stress relaxation the dominant effect is the indirect traction load.

a)   b)
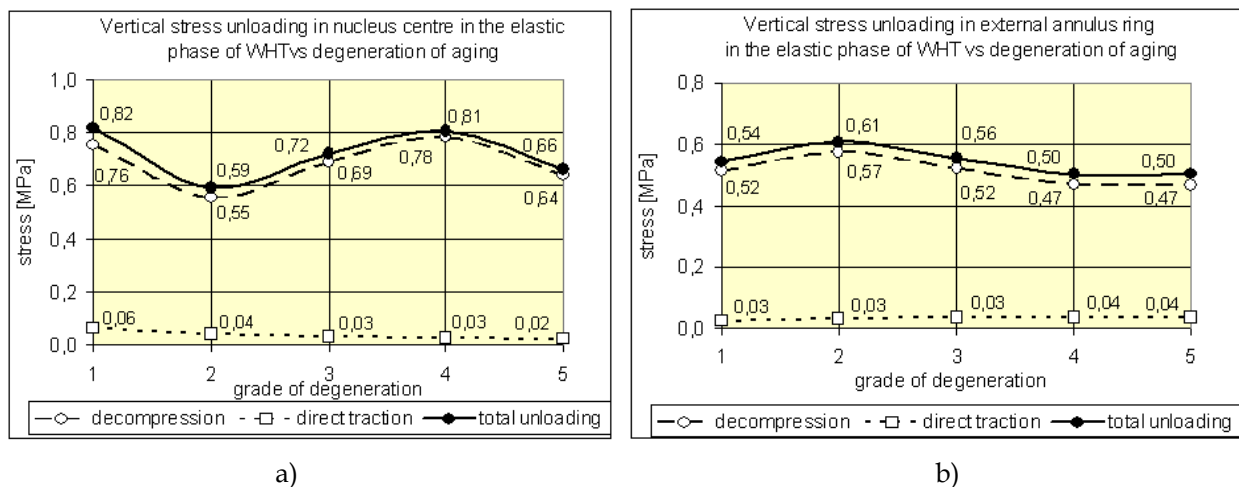
Fig. 10. Stress unloading effect of WHT a) in nucleus centre and b) in the external annulus (Kurutz and Oroszváry, 2010).

It can be concluded that direct traction load with extra lead weights influences mainly the deformations that are responsible for nerve release, while stress relaxation is influenced mainly by the indirect traction load. The traction effect can be increased by applying larger extra lead weights.

7. Conclusion

After a short survey of the structural anatomy and biomechanics of healthy and degenerated lumbar spine, FE modeling and a systematic numerical analysis of the main mechanical features of lumbar spine degenerations was investigated to study the age-related and sudden degeneration processes of it. The fact that mildly degenerated segments have the smallest stiffness both in aging and sudden degeneration processes was numerically proved by answering the question why the LBP problems insult so frequently the young adults.

At the beginning of aging degeneration process, the effect of loss of incompressibility of nucleus, later the hardening of nucleus dominated, yielding the smallest compressive

stiffness of disc at mildly degenerated state. In sudden degeneration processes the smallest stiffness happened also in mildly degenerated state. The 2100 N/mm stiffness suddenly decreased by 75-80% to 400-500 N/mm for mild, and the 3600 N/mm stiffness decreased by 60-65% to 1300 N/mm for severely degenerated case. Vertical intradiscal stresses showed significant change during aging degeneration, between 0.6-1.6 MPa. Disc deformability and bulging was maximum in mildly degenerated state and decreased during aging by 30-85%, while in sudden degeneration increased suddenly by 200-300%.

As for conclusion, FE simulations of degeneration processes of lumbar segments and discs may help clinicians to understand the initiation and progression of disc degeneration and will help to improve prevention methods and treating tools for regeneration of disc tissues.

In WHT, discs show a bilinear material behaviour with higher resistance in indirect and smaller in direct traction phase. Consequently, although the direct traction load is only 6% of the indirect one, direct traction deformations are 15-90% of the indirect ones, depending on the grade of degeneration. Moreover, the ratio of direct stress relaxation remains equally about 6-8% only. Consequently, direct traction controlled by extra lead weights influences mostly the deformations being responsible for the nerve release; while the stress relaxation is influenced mainly by the indirect traction load coming from the removal of the compressive body weight and muscle forces in the water. A mildly degenerated disc in WHT shows 0.15 mm direct, 0.45 mm indirect and 0.6 mm total extension; and 0.2 mm direct, 0.6 mm indirect and 0.8 mm total posterior contraction. A severely degenerated disc exhibits 0.05 mm direct, 0.05 mm indirect and 0.1 mm total extension; 0.05 mm direct, 0.25 mm indirect and 0.3 mm total posterior contraction. These deformations are related to the instant elastic phase of WHT that are doubled during the creep period of the treatment.

As for conclusion, WHT unloads the compressed disc: extends disc height, decreases bulging, stresses and fiber forces, increases joint flexibility, relaxes muscles, unloads nerve roots, relieves pain and may prevent graver problems. WHT is an effective non-invasive method to treat lumbar discopathy. By the presented numerical analysis its beneficial clinical impacts can be supported, moreover, the treatment could be planned, the magnitudes of extra loads could be determined by considering the patient's clinical status.

8. Acknowledgment

9. References

Acaroglu, E.R., Iatridis, J.C., Setton, L.A., Foster, R.J., Mow, V.C., Weidenbaum, M. (1995). Degeneration and aging affect the tensile behaviour of human lumbar anulus fibrosus, *Spine*, 20(24), 2690-2701.

Adams, M.A., Bogduk, N., Burton, K., Dolan, P. (2002). *The Biomechanics of Back Pain*, Churchill Livingstone, London.

Adams, M.A., Freeman, B.J., Morrison, H.P., Nelson, I.W., Dolan, P. (2000), Mechanical initiation of intervertebral disc degeneration, *Spine,* 25(13), 1625-1636.

Adams, M.A., McNally, D.S., Dolan, P. (1996). Stress distributions inside intervertebral discs. The effects of age and degeneration. *J. Bone Joint Surg. Br.* 78(6), 965-972.

Andersson, G.B., Schultz, A.B., Nachemson, A.L., (1983). Intervertebral disc pressures during traction, *Scand. J. Rehabil. Med.* Suppl. 9, 88-91.

Antosik, T., Awrejcewicz, J., (1999). Numerical and Experimental Analysis of Biomechanics of Three Lumbar Vertebrae, *Journal of Theoretical and Applied Mechanics*, 37(3). 413-434.

Bader, D.L., Bouten, C. (2000). Biomechanics of soft tissues. In: Dvir, Z. (Ed.), *Clinical Biomechanics*, Churchill Livingstone, New York, Edinburgh, London, Philadelphia, 35-64.

Bene, É., (1988). Das Gewichtbad, Zeitschrift für Physikalische Medizin, Balneologie, *Medizinische Klimatologie*. 17, 67-71.

Bene É., Kurutz, M., (1993). Weightbath and its biomechanics, (in Hungarian), *Orvosi Hetilap*, 134. 21. 1123-1129.

Benzel, E.C.: *Biomechanics of Spine Stabilization,* (2001). American Association of Neurological Surgeons, Rolling Meadows, Illinois.

Bogduk, N., Twomey, L.T. (1987). *Clinical Anatomy of the Lumbar Spine,* Churchill Livingstone, New York.

Cassinelli, E., Kang, J.D. (2000). Current understanding of lumbar disc degeneration, *Operative Techniques in Orthopaedics*, 10(4), 254-262.

Cheung, J.T.M., Zhang, M., Chow, D.H.K., (2003). Biomechanical Responses of the Intervertebral Joints to Static and Vibrational Loading: a Finite Element Study, *Clinical Biomechnaics*, 18(9), 790-799.

Denoziere, G., (2004). *Numerical Modeling of Ligamentous Lumbar Motion Segment*, Master thesis, Georgia Institute of Technology, 148 p.

Denoziere, G., Ku, D.N., (2006). Biomechanical Comparison Between Fusion of Two Vertebrae and Implantation of an Artificial Intervertebral Disc, *Journal of Biomechanics,* 39(4), 766-775.

Dolan, P., Adams, M.A. (2001). Recent advances in lumbar spinal mechanics and their significance for modelling, *Clinical Biomechanics, 16(Suppl.),* S8-S16.

Dvir, Z. (2000). *Clinical Biomechanics,* Churchill Livingstone, New York, Edinburgh, London, Philadelphia.

Ferguson, S.J., Steffen, T. (2003). Biomechanics of the aging spine, *European Spine Journal*, Suppl 2, S97-S103.

Goel, V.K., Monroe, B.T., Gilbertson, L.G., Brinckmann, P. (1995). Interlaminar shear stresses and laminae separation in the disc. Finite element analysis of the L3-L4 motion segment subjected to axial compressive loads. *Spine*, 20(6), 689-698.

Kurutz, M. (2006a). Age-sensitivity of time-related in vivo deformability of human lumbar motion segments and discs in pure centric tension, *Journal of Biomechanics, 39*(1), 147-157.

Kurutz, M., (2006b). In vivo age- and sex-related creep of human lumbar motion segments and discs in pure centric tension, *Journal of Biomechanics, 39*(7), 1180-9.

Kurutz, M. (2010). Finite element modeling of the human lumbar spine, In: Moratal, D. (ed.): *Finite Element Analysis*, SCIYO, Rijeka, 690 p., 209-236.

Kurutz, M, Bender, T. (2010). Weightbath hydrotraction treatment: application, biomechanics and clinical effects, *Journal of Multidisciplinary Healthcare*, 2010(3), 19-27.

Kurutz, M., Oroszváry, L. (2010). Finite element analysis of weightbath hydrotraction treatment of degenerated lumbar spine segments in elastic phase, *Journal of Biomechanics,* 43(3), 433-441.

Kurutz, M., Tornyos, Á., (2004). Numerical simulation and parameter identification of human lumbar spine segments in traction, In: Bojtár I. (ed.): *Proc. of the First Hungarian Conference on Biomechanics*, Budapest, Hungary, June 10-11, 2004, ISBN 963 420 799 5, 254-263.

Kurutz, M., Bene É., Lovas, A., (2003). In vivo deformability of human lumbar spine segments in pure centric tension, measured during traction bath therapy, *Acta of Bioengineering and Biomechanics, 5*(1), 67-92.

Lavaste, F., Skalli, W., Robin, S., Roy-Camille, R., Mazel, C., (1992). Three-dimensional Geometrical and Mechanical Modelling of Lumbar Spine, *Journal of Biomechanics*, 25(10), 1153-1164.

McGill, S.M. (2000). Biomechanics of the thoracolumbar spine, In: Dvir, Z. (Ed.), *Clinical Biomechanics*, Churchill Livingstone, New York, Edinburgh, London, Philadelphia, 103-139.

McNally, D.S., Adams, M.A. (1992). Internal intervertebral disc mechanics as revealed by sress profilometry, *Spine*, 17(1), 66-73.

Moll, K., (1956). Die Behandlung der Discushernien mit den sogenannten "Gewichtsbadern", *Contempl. Rheum., 97*, 326-329.

Moll, K., (1963). The role of traction therapy in the rehabilitation of discopathy, *Rheum. Balneol. Allerg., 3,* 174-177.

Mosekilde, L. (2000). Age-related changes in bone mass, structure, and strength effects of loading, *Zeitschrift für Rheumatologie*, 59(Suppl.1), 1-9.

Nachemson, A.L. (1981). Disc pressure measurements, *Spine,* 6(1), 93-97.

Natarajan, R.N., Williams, J.R., Andersson, G.B., (2004). Recent advances in analytical modelling of lumbar disc degeneration. *Spine*, 29(23), 2733-2741.

Noailly, J., Wilke, H.J., Planell, J.A., Lacroix, D., (2007). How Does the Geometry Affect the Internal Biomechanics of a Lumbar Spine Bi-segment Finite Element Model? Consequences on the Validation Process, *Journal of Biomechanics*, 40(11), 2414-2425.

Oláh, M., Molnár, L., Dobai, J., Oláh, C., Fehér, J., Bender, T., (2008). The effects of weightbath traction hydrotherapy as a component of complex physical therapy in disorders of the cervical and lumbar spine: a controlled pilot study with follow-up, *Rheumatology International*, 28(8), 749-756.

Panjabi, M.M., Oxland, T., Takata, K., Goel, V., Duranceau, J., Krag, M., (1993). Articular Facets of the Human Spine, Quantitative Three-dimensional Anatomy, *Spine*, 18(10), 1298-1310.

Ramos, G., Martin, W., (1994). Effects of vertebral axial decompression on intradiscal pressure, *Journal of Neurosurgery.* 81(3), 350-353.

Rohlmann, A., Zander, T., Schmidt, H., Wilke, H.J., Bergmann, G., (2006). Analysis of the influence of disc degeneration on the mechanical behaviour of a lumbar motion segment using the finite element method, *Journal of Biomechanics,* 39(13), 2484-2490.

Sato, K., Kikuchi, S., Yonezawa, T. (1999). In vivo intradiscal pressure measurement in healthy individuals and in patients with ongoing back problems, *Spine,* 24(23), 2468-2474.

Schmidt, H., Heuer, F., Simon, U., Kettler, A., Rohlmann, A., Claes, L., Wilke, H.J., (2006). Application of a New Calibration Method for a Three-dimensional Finite Element Model of a Human Lumbar Annulus Fibrosus, *Clinical Biomechanics*, 21(4), 337-344.

Schmidt, H., Kettler, A., Rohlmann, A., Claes, L., Wilke, H,J.. (2007). The Risk of Disc Prolapses With Complex Loading in Different Degrees of Disc Degeneration - a Finite Element Analysis, *Clinical Biomechanics*, 22(9), 988-998.

Shirazi-Adl, A., (1989). On the Fibre Composite Material Models of the Annulus – Comparison of Predicted Stresses. *Journal of Biomechanics*, 22(4), 357-365.

Shirazi-Adl, S.A., Shrivastava, S.C., Ahmed, A.M., (1984). Stress Analysis of the Lumbar Disc-body unit in Compression. A Three-dimensional Nonlinear Finite Element Study, *Spine*, 9(2), 120-34.

Shirazi-Adl, A., Ahmed, A.M., Shrivastava, S.C., (1986). A Finite Element Study of a Lumbar Motion Segment Subjected to Pure Sagittal Plane Moments, *Journal of Biomechanics*, 19(4), 331-350.

White, A. A., Panjabi, M. M. (1990). *Clinical Biomechanics of the Spine*, Lippincott Williams and Wilkins, Philadelphia, etc.

Williams, J.R., Natarajan, R.N., Andersson, G.B.J., (2007). Inclusion of Regional Poroelastic Material Properties Better Predicts Biomechanical Behaviour of Lumbar Discs Subjected to Dynamic Loading, *Journal of Biomechanics*, 40(9), 1981-1987.

Zander, T., Rohlmann, A., Bergmann, G., (2004). Influence of Ligament Stiffness on the Mechanical Behaviour of a Functional Spinal Unit, *Journal of Biomechanics,* 37(7), 1107-1111.
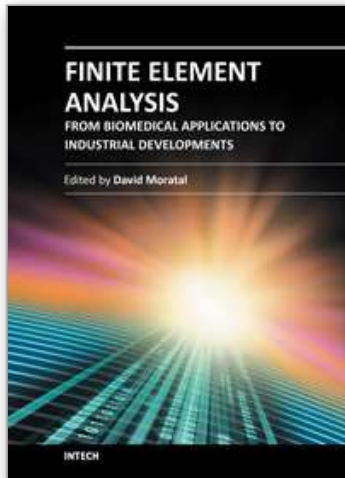
Finite Element Analysis - From Biomedical Applications to Industrial Developments
Edited by Dr. David Moratal

Finite Element Analysis represents a numerical technique for finding approximate solutions to partial differential equations as well as integral equations, permitting the numerical analysis of complex structures based on their material properties. This book presents 20 different chapters in the application of Finite Elements, ranging from Biomedical Engineering to Manufacturing Industry and Industrial Developments. It has been written at a level suitable for use in a graduate course on applications of finite element modelling and analysis (mechanical, civil and biomedical engineering studies, for instance), without excluding its use by researchers or professional engineers interested in the field, seeking to gain a deeper understanding concerning Finite Element Analysis.

How to reference

In order to correctly reference this scholarly work, feel free to copy and paste the following:

Márta Kurutz and László Oroszváry (2012). Finite Element Modeling and Simulation of Healthy and Degenerated Human Lumbar Spine, Finite Element Analysis - From Biomedical Applications to Industrial Developments, Dr. David Moratal (Ed.), ISBN: 978-953-51-0474-2, InTech, Available from: http://www.intechopen.com/books/finite-element-analysis-from-biomedical-applications-to-industrial-developments/finite-element-modeling-and-simulation-of-healthy-and-degenerated-human-lumbar-spine

INTECH
open science | open minds